JOURNAL OF AIRCRAFT
Vol. 29, No. 3, May–June 1992

# Downwash for Joined-Wing Airframe with Control Surface Deflections

John E. Burkhalter,* Donald J. Spring,† and M. Kent Key‡
*Auburn University, Auburn, Alabama 36849*

**An experimental and theoretical investigation of the downwash effects for a joined-wing aircraft was conducted. The investigation included the development of an analytical technique using control surface deflections of both the fore and aft wings instead of the usual tail deflection classical approach. Modifications to the basic equations are presented followed by a comparison with experimental data to validate the procedure. The results indicate differences between experiment and the resulting semiempirical method of less than 12%.**

## Nomenclature

$a$ = aircraft lift-curve slope $\partial C_L/\partial\alpha$, deg$^{-1}$
$C_D$ = drag coefficient
$C_{D0}$ = aircraft drag coefficient for zero aircraft lift
$C_L$ = aircraft lift coefficient
$C_M$ = aircraft pitching moment coefficient
$C_{MAC,t}$ = tail pitching moment coefficient for zero tail lift
$C_{M,AW}$ = aft-wing pitching moment coefficient
$C_{M0}$ = pitching moment coefficient for a wing at zero lift
$C_{M0,WB}$ = forward wing-body pitching moment coefficient for a zero lift condition
$C_{M\alpha}$ = pitching moment slope for the complete aircraft $\partial C_M/\partial\alpha$, deg$^{-1}$
$c$ = mean aerodynamic chord length, ft
$h$ = horizontal center of gravity position (fraction of mean aerodynamic chord)
$h_n$ = horizontal neutral point of aircraft (fraction of mean aerodynamic chord)
$i$ = incidence angle, measured relative to the zero lift line
$i_{GEO}$ = incidence angle, measured relative to the fuselage bottom surface, deg
$i_{\delta=0}$ = geometric incidence angle, formed by the chordline and the fuselage bottom surface (no control surface deflections), deg
$j$ = variable used to increment the change in incidence produced by the number of incremental deflections made relative to the zero deflection reference
$l_{AW}$ = distance between the center of gravity and aft-wing aerodynamic center, ft
$l'_{AW}$ = distance between the forward wing-body aerodynamic center and aft-wing aerodynamic center, ft
$S$ = forward wing reference area, ft$^2$
$V_H$ = horizontal tail volume ratio $S_{AW}l_{AW}/Sc$
$V'_H$ = horizontal tail volume ratio $S_{AW}l'_{AW}/Sc$
$V_{Hn}$ = horizontal tail volume ratio, when $h = h_n$
$V_V$ = vertical tail volume ratio, $z_{AW}S_{AW}/Sc$
$V'_V$ = vertical tail volume ratio $S_{AW}z'_{AW}/Sc$
$V_{Vn}$ = vertical tail volume ratio, when $z = z_n$
$z$ = vertical distance between the center of gravity and the mean aerodynamic center of the wing, ft
$z_n$ = vertical neutral point position for the aircraft (fraction of mean aerodynamic chord)
$\alpha_{L0}$ = zero lift angle of attack for a Göettingen 801 wing, deg
$\alpha_{L0,WB\text{-}GEO}$ = zero lift angle of attack for the forward wing body, deg
$\alpha_{WB\text{-}GEO}$ = forward wing-body geometric angle of attack, deg
$\Delta i_{AW,\delta\neq0}$ = incidence angle change due to a zero lift line rotation caused by an incremental control surface deflection, deg
$\delta_e$ = elevator deflection, deg
$\varepsilon$ = fluid downwash angle, deg
$\varepsilon_0$ = fluid downwash angle when aircraft lift is zero, deg
$\Psi$ = shorthand notation for the angle $\alpha_{WB}(1 - \partial\varepsilon/\partial\alpha) - \varepsilon_0$, deg

*Subscripts*

AW = aft wing
AW-BODY = aft wing body
$t$ = tail
W = wing
WB = wing body

## Introduction

THE joined-wing aircraft, because of the "truss" arrangement, has shown considerable promise of increased payload, decrease in the size requirements for the aircraft, and lower production costs. This concept incorporates two wings in which the forward wing is swept back with positive dihedral to join the aft wing, which is swept forward with anhedral, usually from the top of the vertical stabilizer forming a diamond or "truss" arrangement as seen in Fig. 1. This concept was developed and patented by Wolkovitch[1] in 1976 and an excellent overview of the joined-wing concept, with its advantages and an extensive list of references can be found in Ref. 2. Many others have studied both the structural and aerodynamic advantages in both analytical and experimental investigations;[3-6] among these was a 1984 NASA effort to design a joined-wing demonstrator aircraft that included a validating wind-tunnel test.[7-9] In these theoretical and experimental studies, neither the determination of the downwash characteristics from this unique wing configuration, nor how to determine the downwash from either the basic downwash equations[10] or from the wind-tunnel data were discussed.

Received Jan. 26, 1991; revision received May 17, 1991; accepted for publication May 17, 1991. 

*Associate Professor, Aerospace Engineering Department. Senior Member AIAA.
†Associate Professor, Aerospace Engineering Department. Associate Fellow AIAA
‡Graduate Research Assistant, Aerospace Engineering Department; currently, Aerospace Engineer, Nichols Research, Inc., Huntsville, AL.

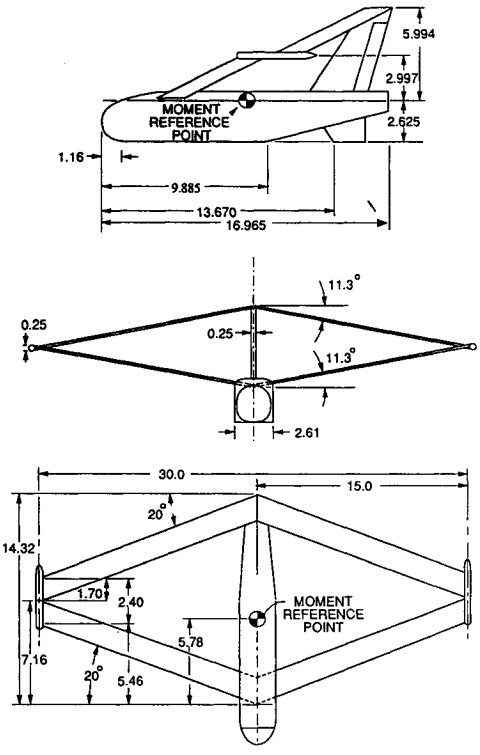


**Fig. 1 Schematic of wind-tunnel model.**

The present investigation was designed to extend the basic downwash equations to account for the downwash from the forward wing as well as the effect of the upwash from the rear wing. The resulting semiempirical equations were validated through a series of low-speed wind-tunnel tests utilizing the baseline model shown in Fig. 1. The test included the body with forward wing, body with aft wing, and the complete configuration. Deflections of control surfaces located on both the forward and aft wing were used for the downwash determination, rather than using the tail deflection alone, which is the usual case.

## Theory

### Nonsimplified Static Stability Equations

While the static stability equations for typical aircraft configurations are well documented and available in Ref. 10, development procedures and underlying assumptions incorporated to simplify the mathematical model for application to a joined-wing aircraft as opposed to the "typical aircraft" were analyzed in the present study. The joined-wing aircraft does not represent a typical aircraft, however, the mathematical equations used to describe the forces and moments produced by a joined-wing aircraft are well represented by the classical forms of the static stability equations. In the present study, careful consideration was given to the simplifications commonly used and their applicability to a generic joined-wing aircraft. Primary emphasis was placed on the development of a set of equations that best describe the aircraft's tendency (or lack thereof) to return to an equilibrium attitude after a disturbance is encountered. This requirement implies that the aircraft have pitch, yaw, and roll stability characteristics conducive to a controllable aircraft. The scope of the present investigation was limited to static pitch stability.

The wing-body moment equation in coefficient form is

$$C_{M,WB} = C_{M0,WB} + [C_{L,WB}\cos\alpha_{WB} + C_{D,WB}\sin\alpha_{WB}](h - h_{n,WB}) + [C_{D,WB}\cos\alpha_{WB} - C_{L,WB}\sin\alpha_{WB}](z - z_{n,WB}) \quad (1)$$

Three basic assumptions are generally applied to Eq. (1) to simplify its form. For small angles of attack, the sine and cosine of the angle of attack are approximated by $\cos\alpha_W = 1.0$ and $\sin\alpha_W = \alpha_W$. For this joined-wing analysis, however, these simplifications are not necessary and will not be used. In addition to the small angle approximation, the vertical distance separating the neutral point and center of gravity is usually set to zero. Thus, terms in Eq. (1) multiplied by $(z - z_{n,WB})$ are usually neglected. For the joined-wing aircraft, the vertical distance between the neutral point and center of gravity may not be negligible and, thus, these terms are retained. Another simplification associated with conventional aircraft is to assume the $C_{D,WB}\sin\alpha_{WB}$ is small in comparison to $C_{L,WB}$. This final simplification is applicable to most joined-wing aircraft, but will not be implemented in the present analysis.

The addition of the aft wing (to the wing and body combination) increases the complexity of the equations describing the aircraft pitching moment. Additionally, mutual flowfield interference effects, controlled by the aft wing placement, require careful consideration to minimize adverse flight characteristics. For the aft wing, the moment produced about the center of gravity is expressed in coefficient form as

$$C_{M,AW} = -[C_{L,AW}\cos(\alpha_{WB} - \varepsilon) + C_{D,AW}\sin(\alpha_{WB} - \varepsilon)](l_{AW}S_{AW}/cS) + [C_{D,AW}\cos(\alpha_{WB} - \varepsilon) - C_{L,AW}\sin(\alpha_{WB} - \varepsilon)] \cdot (z_{AW}S_{AW}/cS) + C_{MAC,AW} \quad (2)$$

This equation accounts for the net downwash seen by the aft wing due to the forward wing set. It is possible that the aft wing could produce upwash that would influence the flow about the forward wing, but the downwash angle $\varepsilon$ presented in Eq. (2) represents the net downwash of the combined influences of both wing sets. Substitution of equations representing the horizontal and vertical tail volume into Eq. (2) results in further simplification.

From Fig. 2, for no control surface deflection on the aft wing, the lift coefficient for the aft wing can be written as

$$C_{L,AW} = a_{AW}\alpha_{AW} = a_{AW}(\alpha_{WB} - \varepsilon - i_{AW}) \quad (3)$$

The downwash angle $\varepsilon$ is approximated by a linear function of $\alpha_{WB}$ and may not hold near the wing tips, but sufficient accuracy over the majority of the span will be achieved with the linear approximation.

Thus far, equations have been developed for specific aircraft components. In addition, the aft wing equations and their dependency on $\alpha_{WB}$ have been addressed. The total lift (complete aircraft) is determined by summing the lift contributions of the forward wing-body combination with the aft wing and using Eq. (3) may be written in coefficient form as

$$C_L = a_{WB}\alpha_{WB}[1 + (a_{AW}S_{AW}/a_{WB}S)(1 - \partial\varepsilon/\partial\alpha)] - a_{AW}(S_{AW}/S)(\varepsilon_0 + i_{AW}) \quad (4)$$

The aircraft lift curve slope is determined by taking the derivative of Eq. (4) with respect to $\alpha_{WB}$ so that replacing $C_L$ by $a\alpha$, results in an equation relating the forward wing-body angle of attack to the complete aircraft angle of attack:

$$\alpha = \alpha_{WB} - (a_{AW}S_{AW}/aS)(\varepsilon_0 + i_{AW}) \quad (5)$$

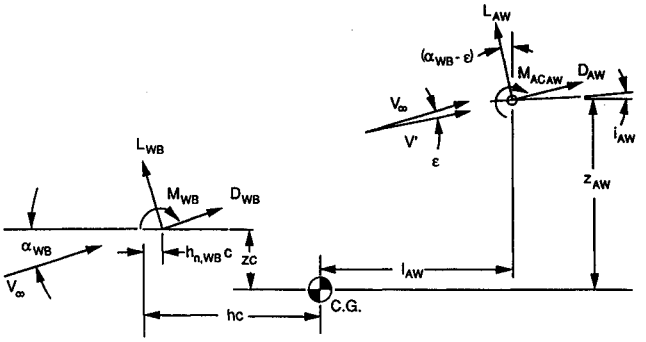


**Fig. 2 Coordinate system and schematic of forward and aft wing locations.**

The aircraft pitching moment equation is determined by combining Eqs. (2) and (3) with a substitution for $C_{L,\mathrm{WB}}$ being made possible by the use of $a_{\mathrm{WB}}\alpha_{\mathrm{WB}}$, resulting in

$$\begin{aligned} C_M &= C_{MAC,\mathrm{AW}} + C_{M0,\mathrm{WB}} + (a_{\mathrm{WB}}\alpha_{\mathrm{WB}}\cos\alpha_{\mathrm{WB}} \\ &+ C_{D,\mathrm{WB}}\sin\alpha_{\mathrm{WB}})(h - h_{n,\mathrm{WB}}) \\ &+ (C_{D,\mathrm{WB}}\cos\alpha_{\mathrm{WB}} - a_{\mathrm{WB}}\alpha_{\mathrm{WB}}\sin\alpha_{\mathrm{WB}})(z - z_{n,\mathrm{WB}}) \\ &+ \{V_V C_{D,\mathrm{AW}} - V_H[a_{\mathrm{AW}}\alpha_{\mathrm{WB}}(1 - \partial\varepsilon/\partial\alpha) \\ &- a_{\mathrm{AW}}(\varepsilon_0 + i_{\mathrm{AW}})]\}\cos[\alpha_{\mathrm{WB}}(1 - \partial\varepsilon/\partial\alpha) - \varepsilon_0] \\ &- \{V_H C_{D,\mathrm{AW}} + V_V[a_{\mathrm{AW}}\alpha_{\mathrm{WB}}(1 - \partial\varepsilon/\partial\alpha) \\ &- a_{\mathrm{AW}}(\varepsilon_0 + i_{\mathrm{AW}})]\}\sin[\alpha_{\mathrm{WB}}(1 - \partial\varepsilon/\partial\alpha) - \varepsilon_0] \end{aligned} \tag{6}$$

By setting $\alpha = 0$ in Eq. (5), then solving for $\alpha_{\mathrm{WB}}$ and substituting the result into Eq. (6), the pitching moment $C_{M0}$ may be written independent of the angle of attack. When allowances are made for $V_H$ and $V_V$ to vary with center of gravity shifts, and noting that changes in $C_{M0}$ are independent of changes in center of gravity position, the resulting equation for $C_{M0}$ is

$$\begin{aligned} C_{M0} &= C_{M0,\mathrm{WB}} + C_{MAC,\mathrm{AW}} + \{V'_V C_{D,\mathrm{AW}} \\ &- V'_H[(aS)^{-1}a^2_{\mathrm{AW}}S_{\mathrm{AW}}(\varepsilon_0 + i_{\mathrm{AW}})(1 - \partial\varepsilon/\partial\alpha) \\ &- a_{\mathrm{AW}}(\varepsilon_0 + i_{\mathrm{AW}})]\}\{\cos[(aS)^{-1}a_{\mathrm{AW}}S_{\mathrm{AW}}(\varepsilon_0 + i_{\mathrm{AW}}) \\ &\cdot (1 - \partial\varepsilon/\partial\alpha) - \varepsilon_0]\} - \{V'_H C_{D,\mathrm{AW}} \\ &+ V'_V[(aS)^{-1}a^2_{\mathrm{AW}}S_{\mathrm{AW}}(\varepsilon_0 + i_{\mathrm{AW}}) \\ &\cdot (1 - \partial\varepsilon/\partial\alpha) - a_{\mathrm{AW}}(\varepsilon_0 + i_{\mathrm{AW}})]\} \\ &\cdot \{\sin[(aS)^{-1}a_{\mathrm{AW}}S_{\mathrm{AW}}(\varepsilon_0 + i_{\mathrm{AW}}) \\ &\cdot (1 - \partial\varepsilon/\partial\alpha) - \varepsilon_0]\} \end{aligned} \tag{7}$$

where, $V'_H$ and $V'_V$ signify the condition $h = h_{n,\mathrm{WB}}$ and $z = z_{n,\mathrm{WB}}$ respectively. Equation (7) also shows that $C_{M0}$ is uniquely defined by the aft wing moment equation for the previously mentioned conditions. The aircraft pitching moment slope determined by taking the derivative of Eq. (6) with respect to $\alpha_{\mathrm{WB}}$ warrants expressing the drag coefficient in terms showing a dependency on $\alpha_{\mathrm{WB}}$. Expressing the drag coefficient in terms of the parasite component, independent of $C_L$, and the induced component dependent on $C_L$ yields a parabolic dependency of $C_D$ on $C_L$. This parabolic dependency can also be applied to the forward wing-body and aft wing components resulting in

$$\begin{aligned} C_{M\alpha}\alpha &= \{[a_{\mathrm{WB}} + C_{D,\mathrm{WB}}][(h - h_{n,\mathrm{WB}})\cos\alpha_{\mathrm{WB}} \\ &- (z - z_{n,\mathrm{WB}})\sin\alpha_{\mathrm{WB}}] \\ &+ (\alpha_{\mathrm{WB}})^{-1}[2(C_{D,\mathrm{WB}} - C_{D0,\mathrm{WB}}) - a_{\mathrm{WB}}\alpha^2_{\mathrm{WB}}] \\ &\cdot [(h - h_{n,\mathrm{WB}})\sin\alpha_{\mathrm{WB}} + (z - z_{n,\mathrm{WB}})\cos\alpha_{\mathrm{WB}}] \\ &- [a_{\mathrm{AW}} + C_{D,\mathrm{AW}}][V_V\sin(\Psi) \\ &+ V_H\cos(\Psi)](1 - \partial\varepsilon/\partial\alpha) \\ &+ (\alpha_{\mathrm{AW}})^{-1}[2(C_{D,\mathrm{AW}} - C_{D0,\mathrm{AW}}) \\ &- a_{\mathrm{AW}}\alpha^2_{AW}][V_V\cos(\Psi) \\ &- V_H\sin(\Psi)](1 - \partial\varepsilon/\partial\alpha)\}\alpha \end{aligned} \tag{8}$$

where $\Psi$ and $\alpha_{\mathrm{AW}}$ are defined by

$$\Psi = \alpha_{\mathrm{WB}}(1 - \partial\varepsilon/\partial\alpha) - \varepsilon_0$$

and

$$\alpha_{\mathrm{AW}} = \alpha_{\mathrm{WB}}(1 - \partial\varepsilon/\partial\alpha) - (\varepsilon_0 + i_{\mathrm{AW}})$$

Equations (7) and (8) are added to form the equation defining the aircraft pitching moment. The neutral point location on the aircraft is determined by setting $h = h_n$ and $z = z_n$ for the condition when $C_{M\alpha} = 0$ in Eq. (8). Thus

$$\begin{aligned} h_n &= \{[(a_{\mathrm{WB}} + C_{D,\mathrm{WB}})(z_n - z_{n,\mathrm{WB}})\sin\alpha_{\mathrm{WB}}] \\ &- [(\alpha_{\mathrm{WB}})^{-1}[2(C_{D,\mathrm{WB}} - C_{D0,\mathrm{WB}}) - a_{\mathrm{WB}}\alpha^2_{\mathrm{WB}}] \\ &\cdot (z_n - z_{n,\mathrm{WB}})\cos\alpha_{\mathrm{WB}}] + [(a_{\mathrm{AW}} + C_{D,\mathrm{AW}})(V_{Vn}\sin(\Psi) \\ &+ V_{Hn}\cos(\Psi))(1 - \partial\varepsilon/\partial\alpha)] \\ &- [(\alpha_{\mathrm{AW}})^{-1}[2(C_{D,\mathrm{AW}} - C_{D0,\mathrm{AW}}) - a_{\mathrm{AW}}\alpha^2_{\mathrm{AW}}] \\ &\cdot [V_{Vn}\cos(\Psi) - V_{Hn}\sin(\Psi)](1 - \partial\varepsilon/\partial\alpha)]\} \\ &\cdot \{(a_{\mathrm{WB}} + C_{D,\mathrm{WB}})\cos(\alpha_{\mathrm{WB}}) + (\alpha_{\mathrm{WB}})^{-1} \\ &\cdot [2(C_{D,\mathrm{WB}} - C_{D0,\mathrm{WB}}) - a_{\mathrm{WB}}\alpha^2_{\mathrm{WB}}] \\ &\cdot \sin(\alpha_{\mathrm{WB}})\} + h_{n,\mathrm{WB}} \end{aligned} \tag{9}$$

Equation (9) reveals that the neutral point in the horizontal plane is coupled with the neutral point location in the vertical plane. In addition, to satisfy the condition $C_{M\alpha} = 0$, vertical movements of the center of gravity, horizontal movements of the center of gravity, or a combination of movements in both planes can be employed. In general, only small vertical center of gravity movements would be possible for most aircraft. Therefore, assuming the $z$ position of the center of gravity is fixed, a decoupled solution for $h_n$ is possible. To eliminate $h_{n,\mathrm{WB}}$ and $z_{n,\mathrm{WB}}$ from Eqs. (8 and 9) additional relations must be introduced that allow for the tail volume ratios to vary with center of gravity movements. Changes in the center of gravity in the horizontal and vertical plane are also allowed in this analysis (see Fig. 2).

Finally then, the equation for the pitching moment is

$$C_M = C_{M0} + \{[a_{WB} + C_{D,WB}]\,[(h - h_n)\cos\alpha_{WB} - (z - z_n)\sin\alpha_{WB}] + (\alpha_{WB})^{-1}[2(C_{D,WB} - C_{D0,WB}) - a_{WB}\alpha_{WB}^2]\,[(h - h_n)\sin\alpha_{WB} + (z - z_n)\cos\alpha_{WB}] + [a_{AW} + C_{D,AW}] \cdot (S_{AW}/S)\,[(h - h_n)\cos(\Psi) + (z - z_n)\sin(\Psi)] \cdot (1 - \partial\varepsilon/\partial\alpha) + \{(\alpha_{AW})^{-1}[2(C_{D,AW} - C_{D0,AW}) - a_{AW}\alpha_{AW}^2]\}\,[(S_{AW}/S)\,[(h - h_n)\sin(\Psi) + (z - z_n)\cos(\Psi)]\,(1 - \partial\varepsilon/\partial\alpha)]\}\alpha \quad (10)$$

**Solution Technique to Determine Interference Effects**

For the present analysis three assumptions and one simplification were employed in the derivations: 1) The downwash was assumed to vary linearly with increased angle of attack; 2) the drag variation with angle of attack was assumed to be parabolic; 3) the dynamic pressure seen by the aft wing was assumed to be the same as that seen by the forward wing-body combination; and 4) higher order terms associated with derivatives of pertinent equations were set to zero.

The method employed to determine the magnitude of the downwash involved careful determination of several pertinent angles that acted as a reference providing for comparison of data between "forward wing-body" and "aft wing-body" configurations. Although the method is nonstandard in nature, the technique is sound and will produce results comparable in accuracy to the accepted method. The normal approach utilizing pitching moment data could not be used due to the joined-wing model fabrication limitations. The usual assumption of imposing the requirement that the tail lift equals zero when the tail moment is zero forces the use of a symmetric airfoil. For cambered airfoils $C_{MAC,t}$ is nonzero, requiring the tail to produce a small amount of lift to negate $C_{MAC,t}$. For the present study, an alternative to using standard pitching moment data for downwash was to use lift data. Using lift data generated by control surface deflections, eliminated the requirement that the tail have a symmetric airfoil. For normal aircraft, the usual procedure is to use incidence angle variations of the tail surface to change the zero lift line of the tail relative to the zero lift line of the wing-body combination. A similar effect was achieved by deflecting the control surfaces on the aft wing of the joined-wing aircraft. In doing so, two changes occurred: 1) $C_{MAC,AW}$ became more negative for positive deflections and less negative for negative deflections; and 2) The aft wing zero lift line rotated clockwise for positive deflections and counterclockwise for negative deflections, relative to the wing's chord line. Because the zero lift of the aft wing changes when a control surface deflects, it can be postulated that it also mimics an incidence change. Changes in $C_{MAC,AW}$ are independent of $C_L$ and $\alpha$, and will not influence the results. The normal and the modified approaches both require tail or aft wing influence on the flow about the forward wing-body combination to be zero or remain constant for all configurations tested. An interesting conclusion stems from the influence requirements. The standard techniques maintains a constant airfoil shape (single tail). Thus, there can be no influence on the flowfield surrounding the wing-body combination for this method to be valid. The new technique varies the airfoil shape (family of aft wings) requiring the influence on the flowfield about the forward wing-body combination to remain constant. Therefore, for the new approach to be valid, elevator deflections on the aft wing must not influence or alter the flow about the forward wing-body combination.

**Proposed Methodology**

In order to determine the amount the zero lift line rotates for a given aft wing control surface deflection, a graph of $C_{L,AW\text{-}BODY}$ vs. $\alpha_{GEO}$ must be constructed. A typical family of curves resulting from the graph is depicted in Fig. 3. Because the aft wing must be tested with the body present, a method to eliminate the body influence must be determined. Using Göettingen 801 airfoil data from an alternate source, a reference value for $\alpha_{L0}$ can be determined. Correction techniques used to convert airfoil values of $\alpha_{L0}$ to finite wing values are given in Ref. 11. With the added assumption that the body influence is constant and does not change when a control surface is deflected, a relationship between aft wing incidence and aft wing incidence change can be developed:

$$i_{AW,GEO} = (i_{AW,\delta=0} - \alpha_{L0}) - j\Delta i_{AW,\delta\neq 0} \quad (11)$$

The first term on the right side of Eq. (11) $i_{AW,\delta=0}$, is the angle formed by the chord line of the aft wing and fuselage bottom surface. The next term $\alpha_{L0}$, is the reference value determined from airfoil data (corrected for three-dimensional flow characteristics). The final term is calculated using Fig. 3. The amount each curve is shifted in $\alpha$ (due to an aft wing control surface deflection) should be constant assuming partial stalling of the aft wing does not occur. Thus, for the present analysis, an average rotation of the zero lift line $\Delta i_{AW,\delta\neq 0}$ is used. The sign of the variable $j$ depends on the direction that the control surface is deflected. The variable $j$ is also used to increment the change in incidence produced by the number of incremental deflections made relative to the zero deflection reference ($\delta = 0$: $j = 0$). For example, if the control surface is set to 10 degrees, $j$ would have a value of $-2$. Likewise, if the control surface was set to $-5$ deg, $j$ would equal 1. Noting that the aft wing incidence angle is

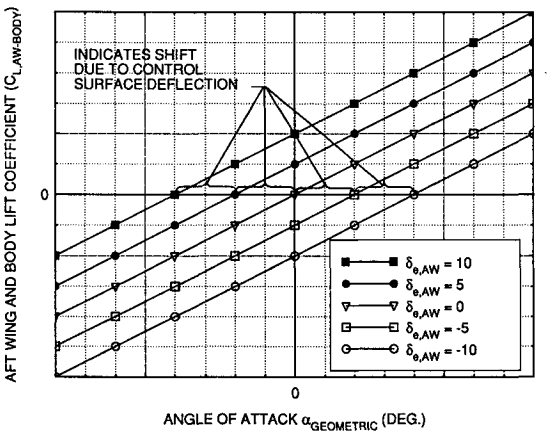


**Fig. 3 Aft wing-body lift coefficient vs geometric angle of attack.**

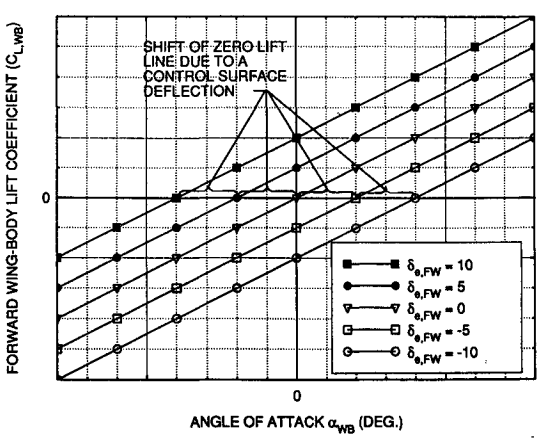


**Fig. 4 Forward wing-body lift coefficient vs wing-body angle of attack.**

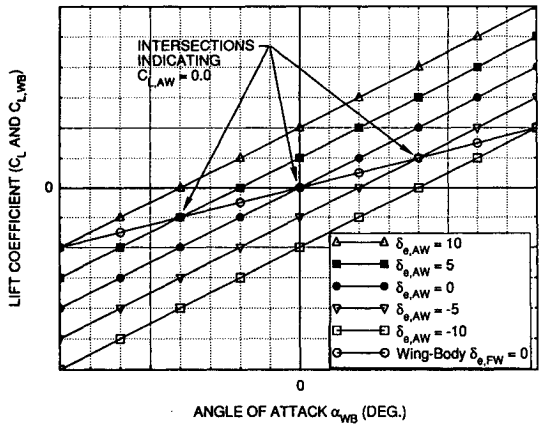


**Fig. 5 Cross-plot of lift coefficient vs angle of attack at several control surface deflections.**

defined by the angle between the zero lift line of the forward wing-body combination and the zero lift line of the aft wing, a transformation from the geometric body reference system to the forward wing-body reference system must be made. The transformation is achieved using

$$i_{AW} = |\alpha_{L0,WB\text{-}GEO}| - i_{AW,GEO} \tag{12}$$

Thus, Eq. (3) can still be used to determine $\varepsilon$.

The value for $\alpha_{WB}$ used in Eq. (6) is determined from the graph of $C_{L,WB}$ vs $\alpha_{WB}$. Again, a typical family of curves, each representing a specific forward wing control surface deflection, is constructed (Fig. 4). The angle that corresponds to $C_{L,WB} = 0$ for each curve is used to determine the zero lift line of the forward wing-body combination relative to $\alpha_{GEO}$:

$$\alpha_{WB} = (\alpha_{WB,GEO} - \alpha_{L0,WB\text{-}GEO}) \tag{13}$$

Therefore, the only unknown in Eq. (3) is $\varepsilon$. By plotting $C_L$ vs $\alpha_{WB}$ for a fixed forward wing control surface deflection, intersections are formed (typical results are given in Fig. 5). The intersections, as discussed earlier, represent the angle of attack at which the aft wing produces no lift. The procedure is repeated for each forward wing control surface setting. The result is a set of downwash equations, each representing a specific forward wing control surface setting.

### Test Procedures

The model configurations used to develop the database were tested at a dynamic pressure of approximately 0.18 psi, which corresponded to a speed of 151 ft/s. The average tunnel Reynolds number was determined to be 128,000.0 based on the mean aerodynamic chord of the wing.

Model configurations required for downwash analysis consisted of forward wing-body, aft wing-body, and complete aircraft. The forward wing-body configuration provided a means of determining $\alpha_{WB}$ when the aft wing lift was zero. It also allowed comparisons between experimental and semiempirical values for $a_{WB}$ to be made. The aft wing-body configuration test results were used in combination with the $\alpha_{L0}$ value determined from Göettingen wing section data so that pseudo-incidence angle settings could be determined. The complete aircraft test results were compared to the forward wing-body results and the angle-of-attack values for zero aft wing lift were obtained. Combining the information ascertained from the forward wing body, aft wing-body, and complete aircraft configuration tests, a systematic solution procedure was possible to determine the downwash influence on the aft wing.

## Results

The solution technique under investigation required a prior knowledge of the lift characteristics associated with the wing sections used in the model design. The zero lift angle of attack value ($\alpha_{L0} = -4.3026$ deg) for the GOE 801 airfoil section used in the tests was extrapolated based on the average tunnel Reynolds Number (128,000) achieved during testing. While airfoil values for $\alpha_{L0}$ do not coincide exactly with three-dimensional wing values, the differences are sufficiently small when the aspect ratio of the wing is large. Thus, no correction was deemed necessary for the present investigation.

The forward wing-body results revealed that flow separation occurred over the control surface deflections of 5, 10, and 15 deg near the zero lift angle of attack. The flow remained separated throughout the pitch polar for the 15-deg setting run. Because of the stall condition, an accurate downwash computation for the 15-deg configuration could not be determined correctly. Flow reattachment occurred for the 10-deg case, a few degrees above the zero lift angle-of-attack attitude, which did provide sufficiently accurate data so that the downwash could be determined. However, the results could not be verified with direct experimental data. Reattachment also occurred for the 5-deg run (very close to $\alpha_{L0}$), which permitted a more accurate determination of $\alpha_{L0}$ for this configuration. The zero lift angles of attack associated with each configuration tested ranged between $-8.0$ deg for a forward wing deflection angle of $-15$, to $-11.7$ deg for a forward deflection of $+5$ deg. All of the $\alpha_{L0}$ angles are relative to the geometric body reference system.

The trends established for the aft wing-body configuration were similar to the forward wing body in that flow separation occurred for many of the runs. The 0-, 5-, 10-, and 15-deg control surface configurations were affected by the separation phenomenon locally close to $\alpha_{L0}$. Of the four configurations, only the 10- and 15-deg setting runs were deleted from the analysis. The decision to delete the two runs was based on the fact that an accurate pseudo-incidence angle of the aft wing could not be guaranteed. The zero lift angles of attack ranged between $-4.6$ deg for an aft wing deflection angle of $-15$, to $-8.7$ deg for an aft deflection of $+5$ deg.

The relative differences between the forward wing-body and aft wing-body zero lift angles for a given control surface setting were indicative of the 3-deg geometric incidence difference between the two wings. In addition, the average rottions of the zero lift line caused by an incremental control surface deflection for both configurations were approximately equal. The average rotations induced by incremental control surface deflections were 1.03 and 1.02 deg for the forward wing body and aft wing body, respectively. The close agreement between the two configurations supports the conclusion that the support rods (used during the aft wing-body test phase) did not influence the test results.

The aft wing-body zero lift angle data as previously determined were used in conjunction with the zero lift angle of attack $\alpha_{L0} = -4.30$ deg and the geometric incidence angle

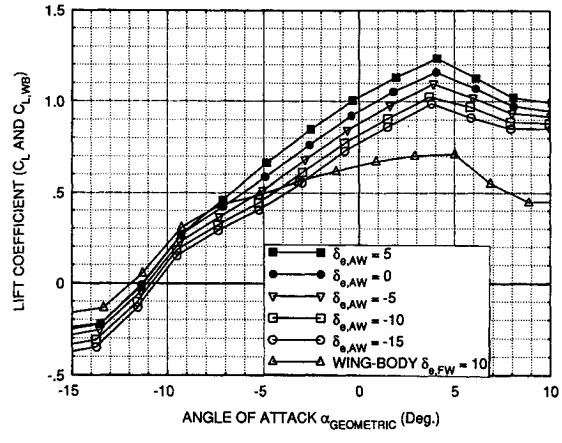


**Fig. 6 Forward wing-body and complete aircraft lift coefficient vs angle of attack for a forward wing control surface setting equal to 10 deg.**

$i_{AW,\delta=0} = 5.25$ deg and substituted into Eq. (11). Maintaining compliance with the linear approximate solution technique, the average incremental rotation $\Delta i_{AW,\delta\neq 0} = 1.02$ deg was used in the analysis. The reason for adhering to the prescribed method was that the region of interest, where downwash information was obtained, showed better compliance with the assumptions made than the $\alpha_{L0}$ test results indicated. Although error was introduced into the analysis, the magnitude of the error remained small. The resulting aft wing incidence settings were then transferred to the forward wing-body reference using Eq. (12).

The final preliminary step required to determine the downwash equation for each forward wing control surface setting was achieved by plotting the forward wing-body and all of the complete aircraft lift curves (for a fixed forward wing control surface setting) on the same graph as shown typically in Fig. 6. The angle locations where the forward wing-body curve intersected the complete aircraft curves corresponded to the zero lift angle of the aft wing. The resulting forward wing-body angle-of-attack values for the condition described above were transferred to the forward wing-body reference using Eq. (13).

Using the data from the above analysis, downwash values $\varepsilon$ were determined from Eq. (3). Downwash plots were also constructed to determine if the assumed linear downwash variation with increases in $\alpha_{WB}$ was valid. Referring to Fig. 7 as typical of the results, the data do show reasonable agreement with the linear assumption. Fluctuations about the mean downwash curve were noted, but the deviances were small considering the accuracy limitations of the test equipment and the linear approximate technique employed for the analysis.

From the wind-tunnel test data, the downwash slopes revealed an increase in downwash slope for negative forward wing control surface deflections. Flow separation noted for positive control surface deflections may partially explain their decreased downwash slope, but further testing must be performed to confirm the true cause. The zero lift downwash ($Y$-intercept) values remained approximately constant for all forward wing control surface settings: with the exception of a $-10$-deg setting. The similarity in the magnitude of the downwash slopes and intercept values suggests that a control surface deflection does not significantly alter the net downwash experienced by the aft wing. Hence, an average downwash equation deduced from the test results can be used for all configuration/control surface combinations.

Ideally, the next logical step would have been to compare the resulting downwash equations to experimental data obtained from an independent source, but data were not available. Thus, an alternate approach was employed using exerimental data combined with the theoretical models that described the joined-wing aircraft being investigated. From Eq. (5), a value for the aft wing lift curve slope was determined for the condition $\alpha = 0$. Subsequently, the aft wing lift curve

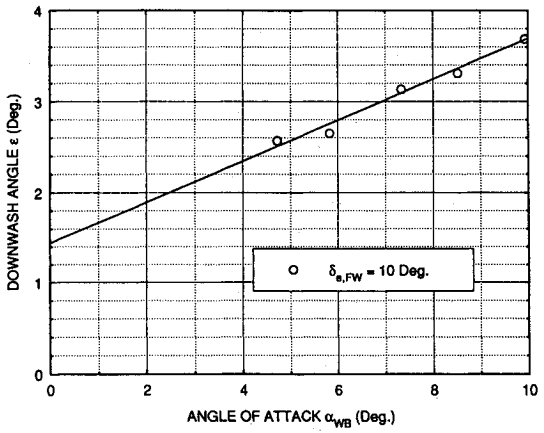


**Fig. 7 Downwash angle vs angle of attack for a forward wing control surface setting equal to 10 deg.**

**Table 1 Average experimental and semiempirical results compared**

| $\delta_{e,FW}$ deg | $\delta_{e,AW}$ deg | $a$ deg$^{-1}$ | Semi-empirical value for $a_{WB}$ deg$^{-1}$ | Experimental value for $a_{WB}$ deg$^{-1}$ | %Diff. in $a_{WB}$ |
|---|---|---|---|---|---|
| 5 | −15 to 5 | 0.0729 | 0.0583 | 0.0519 | 11.62 |
| 0 | | 0.081 | 0.0572 | 0.0534 | 6.87 |
| −5 | | 0.0795 | 0.0531 | 0.0521 | 1.90 |
| −10 | | 0.0814 | 0.0501 | 0.0480 | 4.28 |
| −15 | | 0.0799 | 0.0489 | 0.0500 | −2.22 |

slope value was substituted into Eq. (5) and a semiempirical forward wing-body lift curve slope was obtained. This process accounted for the inclusion of the downwash slope and zero lift intercept. The results obtained from experiment and the semiempirical approch are provided in Table 1. Included in the table are percent difference comparisons of $a_{WB}$ and the complete aircraft lift curve slope values used in Eq. (5).

The agreement between the semiempirical and experimental results support the conclusion that the approach used to determine the downwash behavior of the joined-wing aircraft was credible. Two model geometries did produce percent differences greater than 15%, but both were affected by a localized increase in forward wing-body lift curve slope. The increased differences were expected for this condition because the solution technique did not account for a nonlinear lift curve slope. If a localized slope was determined the differences would have been well below 15%.

Of the forward wing control surface setting groups tested, a forward wing setting of 5 degrees produced the highest average percent difference. The decreased complete aircraft lift curve slopes for these model geometries do indicate a flow separation phenomena. Thus, the experimental values of $a_{WB}$ were lower than the semiempirically determined values.

## Conclusions

The downwash solution technique developed as an analysis tool for joined-wing aircraft was nonstandard, but not less accurate than the standard method discussed previously. In fact, it is possible that the new approach provides better accuracy, but further study is warranted to verify this statement. Accuracy improvements are viable due to the inclusion of a constant aft wing influence on the forward wing body rather than no influence. It also eliminates the size restriction and placement of the aft wing (or tail). The standard technique does not account for aft wing (or tail) influence on the forward wing body restricting size and placement of the aft wing (or tail). Limitations do exist, in spite of the increased flexibility permitted by the new technique.

The use of control surfaces to achieve a pseudoincidence is limited by the control surface's ability to produce enough incidence change required for downwash analysis. The standard technique does not have limitations with regard to incidence setting, provided the model is designed properly. However, both methods are restricted by flow separation. Incidence changes induced by a control surface deflection are severely limited by the control surface's susceptibility to stall. Conversely, if the aft wing (or tail) incidence could be changed, greater incidence variation would be achieved before flow separation becomes an issue. Thus, each method possesses qualities that the other does not. The underlying intention for the development of the new method was not meant to offer a replacement of the standard technique, but rather to provide an alternative approch for downwash analysis when the test article lacked the flexibility required for a standard solution procedure.

## References

[1]Wolkovitch, J., Joined Wing Aircraft, U.S. Patent 3,942,747, March 1976.

[2]Wolkovitch, J., "The Joined Wing: An Overview," *Journal of Aircraft*, Vol. 23, March 1986, pp. 161–178.

[3]Foch, R. J., and Wyatt, R. E., "Low Altitude/Airspeed Unmanned Research Aircraft (LAURA) Preliminary Development," *Proceedings of the Royal Aeronautical Society Conference on Low Reynolds Number Aerodynamics*, 1986.

[4]Hajela, P., and Chen, J. L., "Optimum Structural Sizing of Conventional Cantilever and Joined Wing Configurations Using Equivalent Beam Models," AIAA Paper 86-2653, 1986.

[5]Hollmann, M., "Joined Wing Structures Program," ACA Industries Internal Memorandum, 1986.

[6]White, E. R., "Low-Speed Wind Tunnel Investigation of a Joined-Wing Aircraft Configuration," forthcoming NASA CR.

[7]Wolkovitch, J., "Joined-Wing Research Airplane Feasibility Study," AIAA Paper 84-2471, Nov. 1984, San Diego, CA.

[8]Smith, S. C., Cliff, S. E., and Kroo, I. M., "The Design of a Joined-Wing Flight Demonstrator Aircraft," AIAA Paper 87-2930, Sept. 1987, St. Louis, MO.

[9]Kroo, I. M. and Gallman, J. W., "Aerodynamic and Structural Studies of a Joined Wing Aircraft," AIAA Paper 87-2931, Sept. 1987, St. Louis, MO.

[10]Etkin, B., *Dynamics of Flight Stability and Control*, Wiley, 1982.

[11]Abbott, I. H., and Von Doenhoff, A. E., *Theory of Wing Sections*, Dover, New York, 1959.